Sound and noisy light: Optical control of phonons in photoswitchable structures

Sophia R. Sklan[1] and Jeffrey C. Grossman[2]
[1]*Department of Physics, Massachusetts Institute of Technology, Cambridge, Massachusetts 02139, USA*
[2]*Department of Materials Science and Engineering, Massachusetts Institute of Technology, Cambridge, Massachusetts 02139, USA*
(Received 24 February 2015; revised manuscript received 8 September 2015; published 7 October 2015)

We present a means of controlling phonons via optical tuning. Taking as a model an array of photoresponsive materials (photoswitches) embedded in a matrix, we numerically analyze the vibrational response of an array of bistable harmonic oscillators with stochastic spring constants. Changing the intensity of light incident on the lattice directly controls the composition of the lattice and therefore the speed of sound. Furthermore, modulation of the phonon band structure at high frequencies results in a strong confinement of phonons. The applications of this regime for phonon waveguides, vibrational energy storage, and phononic transistors is examined.

DOI: 10.1103/PhysRevB.92.165107 PACS number(s): 71.36.+c, 61.43.Bn, 63.22.Kn, 64.60.My

Light-matter interactions are of great utility for many of applications. For mechanical vibrations (phonons) these applications encompass creating or destroying phonons using light (optomechanics [1,2], Raman scattering [3–7]), creating or destroying light using phonons (vibronic spectroscopy [8], blackbody radiation [4]), and shifting the refractive index using phonons (acousto-optics [9–11]). However, the last quadrant of this interaction (Table I), the control of phonon properties (e.g., speed of sound c_s) using light remains unexplored. As a result, acousto-optic devices (filters, modulators) are common, whereas controlling phonons remains difficult. Fundamentally, phononic devices require more than the manipulation of phonon populations, but also the tunable manipulation of speed and transmission (phase and amplitude) [12–14]. Optical control, a fast, noncontact technique, is a natural candidate for this. The absence of existing optical control methods for phonons is surprising, as it is well known both that light can tune other material properties (particularly magnetic and electronic properties) by means of inducing structural phase transitions (also known as nonlinear phononics, ionic Raman) [5–7,15–19], and that other signals (pressure, temperature) can control c_s and phonon dispersion (often by phase transitions) [12–14,20–29]. As far as we are aware, the only research that came close to the problem of optical control were Refs. [30–32]. Reference [30] showed that the vibrational properties of a material can be optically switched in photoresponsive liquid crystal polymers, but the optical excitation was intense enough for complete switching, so their focus was rather on the thermal and strain (rather than the optical) tuning of this switching. In contrast, Ref. [31] considered fs laser pulses on bismuth, where photoinduced thermal expansion induces an optical fluence-dependent redshift in some of the phonon modes. The effect is limited by the system melting, as it is an expected signature of materials near a phase transition [33]. It is also similar to the earlier work of Ref. [32] on chalcogenide glasses, where the photosoftening was associated with the approach of a glass-liquid melting transition. There have been other scenarios where optical driving has affected phonon dynamics, such as Ref. [34], but these have been switches between discrete phases (and therefore not tunable) or changed particular resonant modes (i.e., polaritons).

Here, we analyze an approach to controlling c_s via optical intensity. We present a theoretical model of an array of generic photoswitches and demonstrate its use at modulating the phonon band structure, tuning c_s. A numerical analysis of the dynamics reveals additional confinement effects at high frequencies which may prove useful for vibrational energy storage or phononic transistors.

Considering a solid under illumination, there exist three photon-phonon coupling mechanisms. If the basis atoms are polar, then there is a coupling to the electromagnetic field, inducing a localized vibration (direct Raman). If there exists an infrared-active phonon mode, then photons can excite that (ionic Raman). Absent these couplings, light can excite electrons, which excite phonons via electron-phonon coupling (indirect or stimulated Raman). After this initial excitation of a single mode, nonlinearities (electron-phonon coupling or phonon anharmonicity) will disperse this energy into a thermal phonon population. For some materials, these excitations can also induce a structural change, driving the vibrations about some new equilibrium position in ionic Raman or softening a phonon mode in stimulated Raman. Structural changes necessarily change the phonon band structure. To avoid conflating the creation of thermalized phonons and the tuning of the band structure (distinguishable effects for sufficiently weak anharmonicity [35]), we concentrate on nonphotoactive modes and neglect thermalization except for its effect in structural transitions. For consistency, this requires neglecting phonon-phonon couplings, so we concentrate on harmonic phonons. Hence we confine attention to a chain of one-dimensional (1D) simple harmonic oscillators (SHOs) without further loss of generality.

We therefore model a system of n masses ($m \equiv 1$) joined to $N = n + 1$ photoswitchable SHOs (ground state spring constant k_D, excited k_U) with a mechanical driving force $F = F_0 \cos(\omega_0 t)$ at frequency ω_0. Driving pumps a constant supply of energy into the system, so it is helpful to modify the standard clamped boundary conditions ($u_0 = 0 = u_n$, u is displacement) by sandwiching this system between impedance matched systems of n damped (damping rate $\gamma_u \equiv 1$) SHOs ($k = k_D$) and clamping these ends (see Fig. 1). In the more general case, exciting any SHO will not produce switching elsewhere (i.e., no cascades). This is plausible for sufficiently separated photoisomerizing molecules and composite or multilayed structures where only some portion is photosensitive (see the bottom of Fig. 1). However, if there are no photoswitching cascades, then the order and timing of (de)excitation greatly influence the dynamics. To avoid a biased order, switching

TABLE I. The quadrants of light-matter interaction. The first row is light used to control phonons, and the second is sound used to control photons. The first column is changing populations, and the second is changing dispersion.

	Create/destroy	Harden/soften
Photon → phonon	Optomechanics, Raman	?
Phonon → photon	Vibronics, fluorescence	Acousto-optics

is randomized with Poisson statistics (excitation rate $R_D = B_{DU}H$ and deexcitation $R_U = A_{\text{spont}} + B_{UD}H$, where H is photon fluence at a point and A and B are the Einstein coefficients [4]). This is plausible in the case of sufficiently low intensity photoexcitation that shot noise dominates (i.e., individual photon trajectories are relevant, not an ensemble of photons) but is also a technique for ensuring the robustness of the response to changes in the switching order. Switching dynamics is typically complicated, but because the photoexcitation is much faster than any structural rearrangement, these complexities can be neglected (to lowest order) by integrating out the shorter time scales to give

$$\dot{k}(t) = -\gamma_k(k(t) - k_{\text{SS}}(w)), \tag{1}$$

where γ_k determines the rate of the structural reaction [typically $O(\omega_0)$], k_{SS} is the new steady state, and w denotes the stochastic variable describing switching. In principle, a change in the equilibrium position of the lattice is also possible. But our system models a photoswitch embedded in a matrix and does not describe the (realization-dependent) dynamics of modes shorter than one supercell, so this shift is negligible. Hence, the displacement obeys

$$\ddot{u}_i(t) = k_i(t)[u_{i-1}(t) - u_i(t)] + k_{i+1}(t)[u_{i+1}(t) - u_i(t)], \tag{2}$$

where i indexes the site.

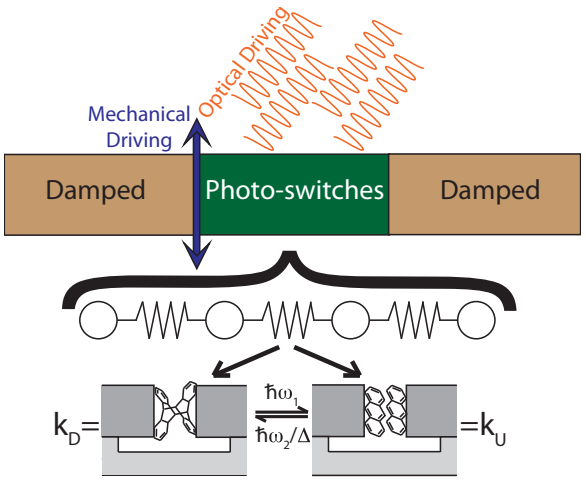

FIG. 1. (Color online) Schematic model of system. Photoswitches (green) sandwiched between damped regions (brown) which are clamped at the far ends. Light (orange curves) is applied to the photoswitches, which are also driven mechanically (blue arrow) to produce phonons. Photoswitches are modeled as a series of 1D SHOs composed of photosensitive materials (e.g., anthracene, see bottom) embedded in a matrix, creating a bistable system with two spring constants.

At steady state this system's eigenmode distribution is solvable using random matrix theory (RMT) [36]. However, this does not describe the effects of changing composition (i.e., traversing the RMT's solution space [37]). Moreover, the eigenfunctions for a single equation can be solved—exponential wave functions when no switching is occurring and modified Bessel functions of imaginary order when switching is occurring—but the inconsistency of this basis set impedes an analytic solution for any nontrivial realization. As such, we integrate the solutions numerically. Switching times/locations, being stochastic, are computed using the Gillespie algorithm [38], and the system can be integrated analytically between switchings. The initial conditions are $u(x,0) = 0 = \dot{u}(x,0)$ and $k_i(0) = k_D$. We use natural units: a is the equilibrium site separation for length and $t_\gamma = 1/\gamma_u$ for time. Using $k_D = 1/t_\gamma^2, k_U = 2/t_\gamma^2, R_U = 1.5/t_\gamma, R_D = 2/t_\gamma$, $F_0 = 1a/t_\gamma^2$, a sample of size $n = 29$ is calculated for interval $T = 100t_\gamma$, giving $u(x,t)$ and $k(x,t)$ at various ω_0.

Given the connection between $u(x,t)$ and $k(x,t)$, plotting them together is useful. Hence we present an unusual visualization scheme in Fig. 2 (alternatively, see the movies in the Supplemental Material [39]). The x axis denotes the position along the chain (0 to N), y time, colored isoval curves are the oscillator amplitude u, and the rectangles are the lattice composition k (gray = ground state, white = excited). For clarity, Fig. 2(a) is supplemented with two subplots. The bottom subplot shows $u(i,t)$ and $k(i \pm 1,t)$ for fixed position i. The side subplot shows $u(x,t_0)$ and $k(x,t_0)$ for fixed time t_0. This is early in our simulation, so the driving signal (from $x = 0$) has not yet propagated along the lattice. Since at low frequencies [Fig. 2(a)] we expect wavelengths $\lambda \gg a$, thus the effect of the switching is a weak perturbation that distorts u. For shorter wavelengths [Fig. 2(b)], the solutions are more sensitive to lattice composition and may be scattered at the composition boundaries (reflecting incident phonons). However, because the lattice composition changes, transmission and reflection fluctuate, giving intervals of strong transmission or reflection. This constitutes a potential mechanism for ultrafast control of thermal conductivity. For even higher frequencies [Fig. 2(c)] the system is above the band edge of one state but not the other [i.e., above $\omega_{\min}(k_{\max}) \equiv \omega_g = 2/t_\gamma$]. This implies that oscillations decay in one state but freely propagate in the other, allowing tunneling. In this case changing composition allows standing waves to be trapped and so could potentially store or steer vibrations. This could also be a form of phononic memory or (detailed later) a phononic transistor. Finally, at frequencies above the band edge of both configurations ($\omega > 2\sqrt{2}/t_\gamma$, not shown), no propagation is possible and the solution decays.

Analyzing $u(x,t;\omega_0)$ shows that photoswitching dramatically affects the transmission and dynamics, but this frequency dependence is also useful for finding the dispersion and thereby c_s. To generate the dispersion, we Fourier transform $u(x,t)$, giving $u(q,\omega)$. The location of the maxima of $u(q,\omega)$ indicates the mode $\omega(q)$ that was excited by driving at ω_0. (To generate a smooth dispersion rather than a series of discrete normal modes, $n = 124$ is used.) This is repeated for $N_{\text{rep}} = 10$ times with $T = 200t_\gamma$ for ergodicity, and ω and q are averaged. Because at high frequencies the waves can be narrowly confined, this will artificially introduce Fourier components near the Γ point. Since these are not features of

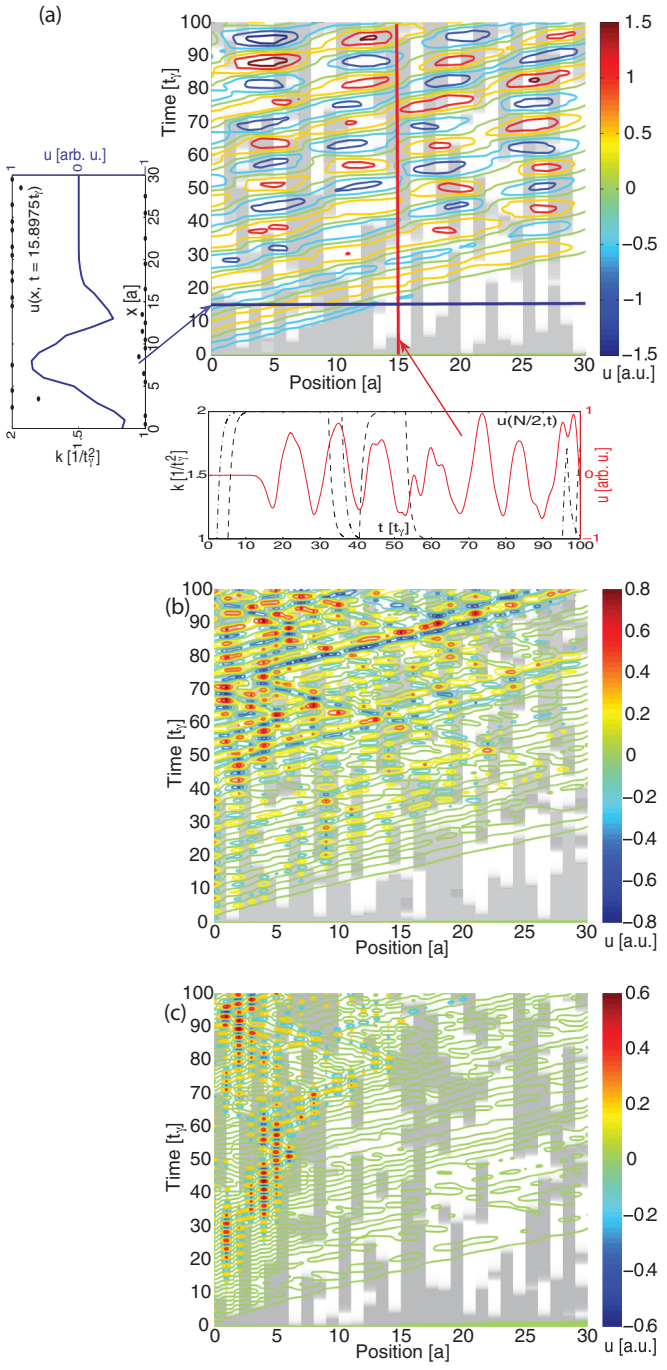

FIG. 2. (Color online) Phonon amplitude under photoswitching. The x axis denotes the distance along the 1D chain, and the y axis denotes time. Contours (colored) are isoval curves of phonon amplitude $u_i(t)$ (see the side bar). Gray segments are the ground state (no illumination), white segments are excited (illuminated), and gradients are transitions. (a) Low frequency ($\omega = 0.5/t_\gamma$). The bottom inset (red, vertical slice) shows $u(N/2,t)$ (red, solid curve) and $k(N/2,t)$,$k(N/2+1,t)$ (black, dashed curves) as a function of time. The side inset (blue, horizontal slice) shows a snapshot $u(x,t_0)$ (blue, solid curve) and $k(x,t_0)$ (black dots) as a function of position. (b) Midfrequency ($\omega = 1.5/t_\gamma$). (c) High frequency ($\omega = 2.5/t_\gamma$).

the wave form itself, but of its confinement, we exclude these terms from the average. Repeating this for multiple frequencies allows us to construct the dispersion, which is repeated for

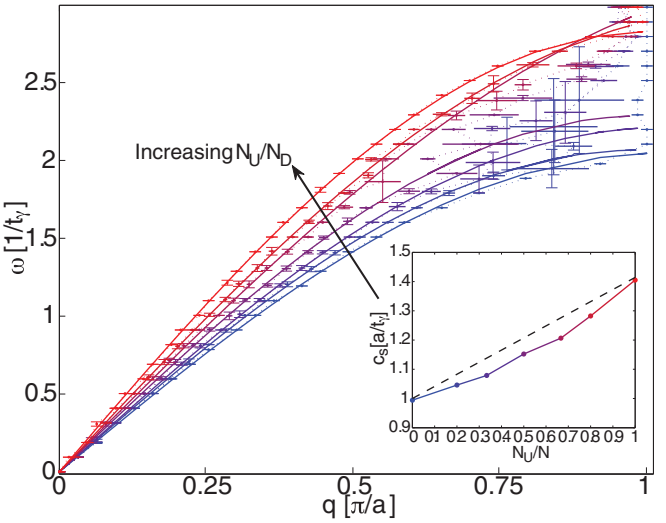

FIG. 3. (Color online) Dispersion $\omega(q)$ for a 1D chain of photoswitches. The color denotes the strength of illumination from blue (no illumination, all in the ground state) through red (full illumination, all in the excited state). Dotted lines and dots (with error bars) indicate numerical results. Solid lines denote fits to the sinusoid dispersion. Inset: Speed of sound as a function of fraction in the excited state. The colored, solid line is the numerical fit (the color corresponds to dispersion) and the black, dashed line is the kinetic model.

various combinations of R_U/R_D in Fig. 3. Note that for points above ω_g (i.e., in the confinement regime), some of the dispersions show a pronounced drop in q. This is an artifact of the exponential decay regions, which lower the effective wavelength. Ergo, this jump is a result of limitations in defining a wavelength for such a heterogeneous system. So when we fit the dispersion $\omega(q;R_U/R_D)$ to a sine curve $c_{s,\mathrm{eff}}\sin(a_{\mathrm{eff}}q)/a_{\mathrm{eff}}$ (the dispersion for a homogeneous 1D chain, $c_{s,\mathrm{eff}}$ and a_{eff} are fitting parameters) it is helpful to exclude these points.

From the fitted dispersion we can extract the effective $c_{s,\mathrm{eff}}$ by expanding for small q, giving (in units of a/t_γ)

$$c_{s,\mathrm{eff}} = 0.997 + 0.177N_U/N + 0.227(N_U/N)^2, \qquad (3)$$

where N_U is the excited state population, $c_{s,D} = 1a/t_\gamma$ is the ground state's speed of sound, and $c_{s,U} = \sqrt{2}a/t_\gamma$ is the excited state's (see Fig. 3 inset). From the master equation

$$\dot{N}_D = -R_D N_D + R_U N_U = -\dot{N}_U, \qquad (4)$$

the steady state compositions are

$$\frac{N_U}{N} = \frac{R_D}{R_D + R_U} = \frac{(g_U/g_D)H}{S(\omega_\nu) + (1 + g_U/g_U)H}, \qquad (5)$$

where $g_{U,D}$ are the mode degeneracies, $S = 2\hbar\omega_\nu^3/\pi c^3$, and ω_ν is the photon frequency (the last relation comes from a detailed balance of the Einstein coefficients [4]). Changing R_U/R_D changes N_U/N_D, so increasing the optical intensity increases the equilibrium population in the excited state (to some limiting fraction given by the mode degeneracies). Therefore,

changing illumination gives direct control of c_s. Now, consider a simple kinetic model where c_s in the ground (excited) state is $c_{s,D}$ ($c_{s,U}$). The average speed for an inhomogeneous system would be the weighted average $c_{s,D}N_D/N + c_{s,U}N_U/N$ or

$$c_s^{(\mathrm{kin})} = c_{s,D} + (c_{s,U} - c_{s,D})N_U/N, \tag{6}$$

i.e., linear with composition. This disagrees with our observed relation, which falls below this kinetic limit except for the homogeneous cases of $N_U/N = 0$ or 1, which agree with the analytic results to within 99% accuracy (see Fig. 3 inset). This is expected, though, as reflections delay a pulse and decrease its effective velocity.

Finally, consider again the confined regime. In the homogeneous cases the transmittivity of the material should be nearly 1 (i.e., no loss) or 0 (i.e., perfect damping) for a sufficiently thick sample. Switching between these compositions (possible when $g_U \gg g_D$ and the photon intensity is large, or stochastically possibly for $R_D > R_U$ and $N \approx g_U/g_D$) allows for illumination controlled switching between transmission and reflection. Dynamically changing R_D/R_U therefore allows for controlled phonon transmission. This switching mechanism is therefore a potential phononic transistor using the optical analog indirect control scheme presented in Ref. [14] (i.e., a light source instead replaces the electromagnet). Such an indirect transistor is more easily tuned than the direct designs, which rely upon phonon-phonon couplings [29] that are not dynamically accessible. To show the feasibility of this proposal, we repeat our calculations for a pulsed illumination [$R_D^{(\mathrm{on})} = 4/t_\gamma$, $R_D^{(\mathrm{off})} = 0$]. Pulse widths are selected such that a homogeneous composition is produced for each state. Since complete, monotonic switching of a sample has the expectation value

$$R_{U,D}\tau_{U,D}^{(N)} = N\sum_1^N \frac{1}{v} = NH_N \approx N\ln N, \tag{7}$$

where H_N is the harmonic function, we use a sample size of $n = 9$ for these simulations (illumination period $200t_\gamma$, dark period $200t_\gamma$, total run time $2000t_\gamma$, $R_D = 4/t_\gamma = 8R_U$). Plotting the amplitude at the far end of the sample (normalized to the maximum amplitude without damping $\max[u_0(L,t)]$) gives Fig. 4 for a $\omega = 2.1/\tau_\gamma$. The horizontal lines indicate the rms average amplitude during each period of darkness or illumination (including switching intervals, therein underestimating the difference). For frequencies below ω_g there is transmission for both states, so the ratio of these averages is nearly 1 (not shown), whereas for frequencies just above ω_g there is a large difference between the states and so a large separation is observed (Fig. 4). As frequency increases above ω_g, transmission drops and the ratio again approaches 1 (not shown). Comparing these results with Fig. 2(c) reveals a crossover from confinement to transmission with increasing photon intensity. For confinement to be effective, there should be narrow domains of the propagating configuration, which is best achieved with weak driving.

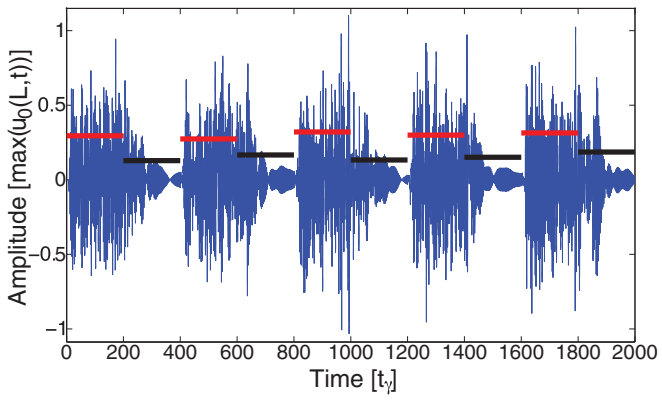

FIG. 4. (Color online) Transmitted signal (amplitude vs time) of photoswitches in a switch/transistor regime. The blue curve is the response, the black curve is the rms average over dark period, and the red curve is the rms average over the illuminated interval. The separation of the black and red curves is the switch's efficacy.

In summary, we have demonstrated an approach controlling the phononic properties of a system, using light to tune the phonon band structure. This reverses the acousto-optic formulation of phonons modulating the index of refraction, and instead light modulates c_s. The shifting of the dispersion that this allows opens several interesting possibilities for phononic devices. Delay lines and, by extension, phase control gates can be constructed by tuning the speed of sound. Thermal conductivity modulation is clearly achievable by the controlled scattering of short-wavelength phonons from the configuration boundaries. Vibrational energy storage or phononic memory are possible in the high frequency regime with phonon confinement under weak optical driving, and under the same regime with strong optical driving, an optophononic switch or indirect phononic transistor is feasible. The control of the speed of sound could also improve the short-term storage (RAM) of phononic information through delay line memory, similar to Ref. [40]. Furthermore, the patterning of photoswitches in a system—or their patterned photoexcitation—allows for real-time, adaptable phononic materials, including phononic crystals and metamaterials. This can be particularly useful (in the confinement regime) for creating waveguides that dynamically control the propagation of phonons or for tuning the thermal conductivity by selectively introducing scatterers. Such an approach would also be experimentally feasible, as an optically controlled bandpass filter was proposed using a superlattice of resonant cavities with chalcogenide glasses in [41] (only light or dark states were simulated and so no intensity-dependent tunability was observed). Similar approaches for experimentally realizing these devices could be achieved by superlattices of photosensitive materials (e.g., photoisomers [30], ionic Raman-active materials [31], photoelastic glasses such as chalcogenides [32]) separated by inactive layers or by embedding these photosensitive materials (particularly photoisomers, which are generally small organic molecules) within an inactive matrix (the scenario illustrated in Fig. 1). Finally, the prevalence of phonon couplings in quantum computing, electronics, phoxonics, and spintronics [42–46] implies that these effects may have further applications in the optical control of a great many signals in a cavalcade of fields.

This material is based upon work supported by the National Science Foundation Graduate Research Fellowship under Grant No. 1122374.

[1] P. F. Cohadon, A. Heidmann, and M. Pinard, Cooling of a Mirror by Radiation Pressure, Phys. Rev. Lett. **83**, 3174 (1999).

[2] C. Höhberger-Metzger and K. Karrai, Cavity cooling of a microlever, Nature (London) **432**, 1002 (2004).

[3] C. V. Raman, A new radiation, Indian J. Phys. **2**, 387 (1928).

[4] R. Loudon, *The Quantum Theory of Light*, 3rd ed. (Oxford University Press, New York, 2001).

[5] C. A. D. Roeser, M. Kandyla, A. Mendioroz, and E. Mazur, Optical control of coherent lattice vibrations in tellurium, Phys. Rev. B **70**, 212302 (2004).

[6] O. Synnergrena, T. N. Hansen, S. Canton, H. Enquist, P. Sondhauss, A. Srivastava, and J. Larsson, Coherent phonon control, Appl. Phys. Lett. **90**, 171929 (2007).

[7] S. Wall, D. Wegkamp, L. Foglia, K. Appavoo, J. Nag, R. F. Haglund Jr., J. Stähler, and M. Wolf, Ultrafast changes in lattice symmetry probed by coherent phonons, Nat. Commun. **3**, 721 (2012).

[8] P. W. Atkins and J. de Paula, *Physical Chemistry*, 8th ed. (Oxford University Press, New York, 2006).

[9] L. Brillouin, Diffusion de la lumière et des rayons X par un corps transparent homogène. Influence de l'agitation thermique, Ann. Phys. (Paris) **17**, 88 (1922).

[10] P. Debye and F. W. Sears, On the scattering of light by supersonic waves, Proc. Natl. Acad. Sci. USA **18**, 409 (1932).

[11] R. Lucas and P. Biquard, Propriétés optiques des milieux solides et liquides soumis aux vibrations élastiques ultra sonores, J. Phys. (Paris) **71**, 464 (1932).

[12] N. Li, J. Ren, L. Wang, G. Zhang, P. Hänggi, and B. Li, Colloquium: Phononics: Manipulating heat flow with electronic analogs and beyond, Rev. Mod. Phys. **84**, 1045 (2012).

[13] M. Maldovan, Sound and heat revolutions in phononics, Nature (London) **503**, 209 (2013).

[14] S. R. Sklan and J. C. Grossman, Phonon diodes and transistors from magneto-acoustics, New J. Phys. **16**, 053029 (2014).

[15] M. Först, C. Manzoni, S. Kaiser, Y. Tomioka, Y. Tokura, R. Merlin, and A. Cavalleri, Nonlinear phononics as an ultrafast route to lattice control, Nat. Phys. **7**, 854 (2011).

[16] A. Subedi, A. Cavalleri, and A. Georges, Theory of nonlinear phononics for coherent light control of solids, Phys. Rev. B **89**, 220301(R) (2014).

[17] E. G. Gamalyn and A. V. Rode, Physics of ultra-short laser interaction with matter: From phonon excitation to ultimate transformations, Prog. Quantum Electron. **37**, 215 (2013).

[18] K. Yonemitsua and K. Nasu, Theory of photoinduced phase transitions in itinerant electron systems, Phys. Rep. **465**, 1 (2008).

[19] S. Wall, D. Prabhakaran, A. T. Boothroyd, and A. Cavalleri, Ultrafast Coupling between Light, Coherent Lattice Vibrations, and the Magnetic Structure of Semicovalent $LaMnO_3$, Phys. Rev. Lett. **103**, 097402 (2009).

[20] N. Sepúlveda, R. Armando, R. Cabrera, and F. Fernández, Young's modulus of thin films as a function of temperature including insulator-to-metal transition regime, Appl. Phys. Lett. **92**, 191913 (2008).

[21] S. Li, X. Ding, J. Ren, X. Moya, J. Li, J. Sun, and E. K. H. Salje, Strain-controlled thermal conductivity in ferroic twinned films, Sci. Rep. **4**, 6375 (2014).

[22] Z. Guo, D. Zhang, and X.-G. Gong, Thermal conductivity of graphene nanoribbons, Appl. Phys. Lett. **95**, 163103 (2009).

[23] X. Li, K. Maute, M. L. Dunn, and R. Yang, Strain effects on the thermal conductivity of nanostructures, Phys. Rev. B **81**, 245318 (2010)

[24] N. Wei, L. Xu, H.-Q. Wang, and J.-C. Zheng, Strain engineering of thermal conductivity in graphene sheets and nanoribbons: A demonstration of magic flexibility, Nanotechnology **22**, 105705 (2011).

[25] K. G. S. H. Gunawardana, K. Mullen, J. Hu, Y. P. Chen, and X. Ruan, Tunable thermal transport and thermal rectification in strained graphene nanoribbons, Phys. Rev. B **85**, 245417 (2012).

[26] R. T. Zheng, J. Gao, J. Wang, and G. Chen, Reversible temperature regulation of electrical and thermal conductivity using liquid—solid phase transitions, Nat. Commun. **2**, 289 (2011).

[27] J. Zhu, K. Hippalgaonkar, S. Shen, K. Wang, Y. Abate, S. Lee, J. Wu, X. Yin, A. Majumdar, and X. Zhang, Temperature-Gated Thermal Rectifier for Active Heat Flow Control, Nano Lett. **14**, 4867 (2014).

[28] F. Li, C. Chong, J. Yang, P. G. Kevrekidis, and C. Daraio, Wave transmission in time- and space-variant helicoidal phononic crystals, Phys. Rev. E **90**, 053201 (2014).

[29] D. Hatanaka, I. Mahboob, K. Onomitsu, and H. Yamaguchi, A phonon transistor in an electromechanical resonator array, Appl. Phys. Lett. **102**, 213102 (2013).

[30] M. Petr, M. E. Helgeson, J. Soulages, G. H. McKinley, and P. T. Hammond, Rapid viscoelastic switching of an ambient temperature range photo-responsive azobenzene side chain liquid crystal polymer, Polymer **54**, 2850 (2013); E. Verploegen, J. Soulages, M. Kozberg, T. Zhang, G. H. McKinley, and P. T. Hammond, Reversible switching of the shear modulus of photoresponsive liquid-crystalline polymers, Angew. Chem. **48**, 3494 (2009).

[31] T. Garl, E. G. Gamaly, D. Boschetto, A. V. Rode, B. Luther-Davies, and A. Rousse, Birth and decay of coherent optical phonons in femtosecond-laser-excited bismuth, Phys. Rev. B **78**, 134302 (2008).

[32] J. Gump, I. Finkler, H. Xia, R. Sooryakumar, W. J. Bresser, and P. Boolchand, Light-Induced Giant Softening of Network Glasses Observed near the Mean-Field Rigidity Transition, Phys. Rev. Lett. **92**, 245501 (2004).

[33] C. Kittel, *Introduction to Solid State Physics*, 8th ed. (Wiley, New York, 2004).

[34] S. L. Johnson, P. Beaud, E. Vorobeva, C. J. Milne, É. D. Murray, S. Fahy, and G. Ingold, Directly Observing Squeezed Phonon States with Femtosecond X-Ray Diffraction, Phys. Rev. Lett. **102**, 175503 (2009).

[35] Thermalization and velocity modulation are distinct effects, assuming sufficiently weak nonlinearity to the lattice. Considering a current of phonons $J = nv$, thermalization will change the number of phonons n while structural changes will change the velocity v. It is only when anharmonicity is so strong that the band structure is intensity dependent that this distinction breaks down. Even then, the use of low amplitude phonons makes this negligible.

[36] F. J. Dyson, The dynamics of a disordered linear chain, Phys. Rev. **92**, 1331 (1953).

[37] Changing compositions is also equivalent to traversing different realizations of a glassy or disordered medium, or taking an ensemble average over disorder.

[38] D. T. Gillespie, Exact stochastic simulation of coupled chemical reactions, J. Phys. Chem. **81**, 2340 (1977).

[39] See Supplemental Material at http://link.aps.org/supplemental/10.1103/PhysRevB.92.165107 for animations of lattice dynamics.

[40] M. V. Wilkes, Computers Then and Now, J. Assoc. Comput. Mach. **15**, 1 (1968).

[41] N. Swinteck, P. Lucas, and P. A. Deymier, Optically tunable acoustic wave band-pass filter, AIP Adv. **4**, 124603 (2014).

[42] A. N. Cleland and M. R. Geller, Superconducting Qubit Storage and Entanglement with Nanomechanical Resonators, Phys. Rev. Lett. **93**, 070501 (2004).

[43] P. Rabl, S. J. Kolkowitz, F. H. L. Koppens, J. G. E. Harris, P. Zoller, and M. D. Lukin, A quantum spin transducer based on nanoelectromechanical resonator arrays, Nat. Phys. **6**, 602 (2010).

[44] Z. M. Zhu, D. J. Gauthier, and R. W. Boyd, Stored light in an optical fiber via stimulated brillouin scattering, Science **318**, 1748 (2007).

[45] T. A. Palomaki, J. W. Harlow, J. D. Teufel, R. W. Simmonds, and K. W. Lehnert, Coherent state transfer between itinerant microwave fields and a mechanical oscillator, Nature (London) **495**, 210 (2013).

[46] S. A. McGee, D. Meiser, C. A. Regal, K. W. Lehnert, and M. J. Holland, Mechanical resonators for storage and transfer of electrical and optical quantum states, Phys. Rev. A **87**, 053818 (2013).